DOI:10.34918/85109

Bartłomiej PYCIŃSKI[1,*], Karolina KOWOL[1], Jan JUSZCZYK[1], Ewa PIĘTKA[1]

Chapter 9. X-RAY MICROTOMOGRAPHY IMAGING OF FRESH AND FORMALIN-FIXED POULTRY HEART

9.1. Introduction

X-ray microtomography (μCT) is an X-ray technique whose popularity and area of application have been increasing in recent years [1]. This imaging allows obtaining three-dimensional images with a resolution of up to micrometers (thus the technique's name). During the imaging, a set of two-dimensional cone-beam projections is acquired. The final three-dimensional (3D) image is reconstructed from the projections. The μCT technique combines features of both classical X-ray (cone beam, planar projections, image magnification) and computed tomography (3D reconstruction). The main feature that distinguishes this technique is the acquisition geometry (Fig. 1), which involves a rotating table with a sample between the X-ray tube and the flat detector. The closer the table is to the tube, the higher the magnification on the detector and the better the final image resolution. Thus, the highest resolution (on the single micrometers level) is only possible with small samples of dimensions up to few centimeters.

μCT is commonly used in life science studies, especially in tissue engineering. Other areas of interest include botany, biotechnology, or chemistry. Besides, it is employed in biomedical engineering, materials science, electronics, and physics. A survey on the application of μCT in these fields was given in [2, 3].

[1] Faculty of Biomedical Engineering, Silesian University of Technology, Zabrze, Poland.
* Corresponding author: bartlomiej.pycinski@polsl.pl.

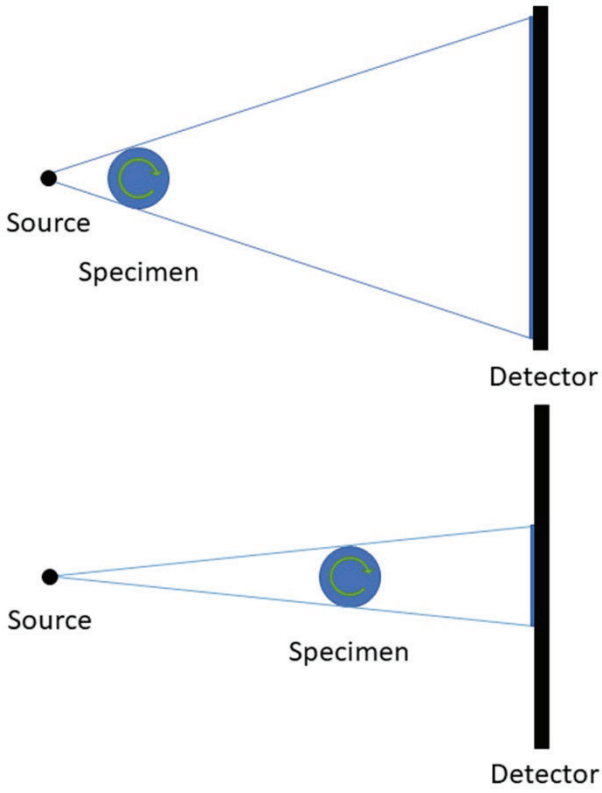

Fig. 1. µCT device components: X-ray source – specimen – detector. The closer the sample is to the source, the greater the magnification of the image
Rys. 1. Elementy aparatu µCT: źródło promieni X – próbka – detektor. Im bliżej źródła jest próbka, tym większe powiększenie obrazu

µCT imaging can also be achieved using a parallel beam of X-rays generated in a synchrotron. Since the X-rays in such machines are monochromatic, the detectors not only measure the intensity of the radiation but also detect the gradient of the phase shift or the transverse Laplacian of the phase [4]. This type of measurement allows for obtaining much higher contrast, especially for soft tissues. [5]. The former µCT technique (based on the X-ray tube) in animal tissue imaging is mainly used for hard tissues (bones, cartilages) or assessment of focal lesions (calcifications, stiff tumors, fibrosis etc). The remaining part of this paper discusses only classical µCT imaging generated by the tube.

It remains an open question whether µCT can – to some extent – replace or complement histopathological imaging. The latter is the gold standard for diagnosing many diseases, but it also has drawbacks: it irreversibly destroys the specimen during preparation and is expensive, and time-consuming. Moreover, few slides are obtained during the preparation, and they are evaluated only in two dimensions. Pathologists have no information about the tissue architecture in 3D space. A solution to this

problem could be so-called 3D histopathology, in which consecutive slices are aligned [6]. However, this is still a relatively uncommon technique [7].

During histological preparation, the specimen is processed in numerous consecutive steps [8]. Immediately after being collected, it is fixed in formaline (4% buffered water solution of formaldehyde). The next steps contain immersion in increasing solutions of propanol or ethanol, then in 100% xylene. The final step is embedding in paraffin, which leads to formaline-fixed, paraffin-embedded (FFPE) samples.

This study aims to compare μCT images of fresh and formalin-fixed (FF) poultry heart specimens. These are preliminary measurements that are currently being developed. Other similar studies have focused on imaging FFPE samples alone or comparing FFPE with FF images [8-11] or on involving staining to enhance tissue contrast [12-14].

9.2. Materials and methods

9.2.1. X-ray imaging

All the images were acquired with the ProCon X-Ray CT-Compact plus system (https://procon-x-ray.de), deployed and adjusted by Casp System. The machine is controlled by a dedicated software provided by the manufacturer. The application allows the manipulation of a wide range image acquisition parameters. The parameters selected for this study are given in Table 1, they follow the Standard Operating Procedure of Microcomputed tomography [15]. No pixel binning was applied. The acquired projections were reconstructed using X-AID v. 2020.3.3, the software that the device manufacturer recommends. The FDK algorithm, the ring artifact correction, and the Hamming filter were used for both examinations to reconstruct final 3D images. The resolution of the reconstructed images was 19.2 μm in all three dimensions.

Table 1

Details of X-ray μCT machine

Voltage [kV]	Current [μA]	Power [W]	Exposure time [s]	FOD [mm]	No of projections	Total duration [h:m:s]
40	160	6.4	2	100.15	2880	3:12:29

9.2.2. Intensity range of μCT reconstructions

In the employed system, the obtained intensity values are represented as 16-bit unsigned integers ranging from 0 to 65 535. They do not directly map onto the Hounsfield scale. Therefore we can directly compare only the results obtained with exactly the same acquisition parameters. In this study, this requirement was fulfilled.

To convert intensity values to Hounsfield units (HU), the μCT system has to be calibrated with a calibration phantom [16]. The phantom consists of a container with water and air. After obtaining final images, HU can be determined according to the equation:

$$\mathrm{HU}(x) = 1000 \cdot \frac{\mu_x - \mu_{\mathrm{H_2O}}}{\mu_{\mathrm{H_2O}} - \mu_{Air}} \quad (1)$$

where μ_x, $\mu_{\mathrm{H_2O}}$, μ_{Air} are the linear attenuation coefficients for the examined voxel, the water and air, respectively.

The values of HU are computed for a specific acquisition parameter set and when they changes, the calibration shall be repeated. The detector's response linearity should also be verified.

9.2.3. Poultry tissue

In the experiments, we used a poultry (hen) heart obtained from a meat store. The organ was stored for 24-48 hours at 4-6°C after the preparation of the hen. Two μCT examinations were performed. The first, without additional preparation, in the horizontal position of the specimen. Then, immediately after imaging, the heart was placed in formalin (4% buffered water solution of formaldehyde) at 20°C for 48 hours. After this time, the heart was picked up, rinsed with tap water, and mildly dried. The second imaging was then performed with identical acquisition parameters as before (Fig. 2). The specimen was disposed of after use.

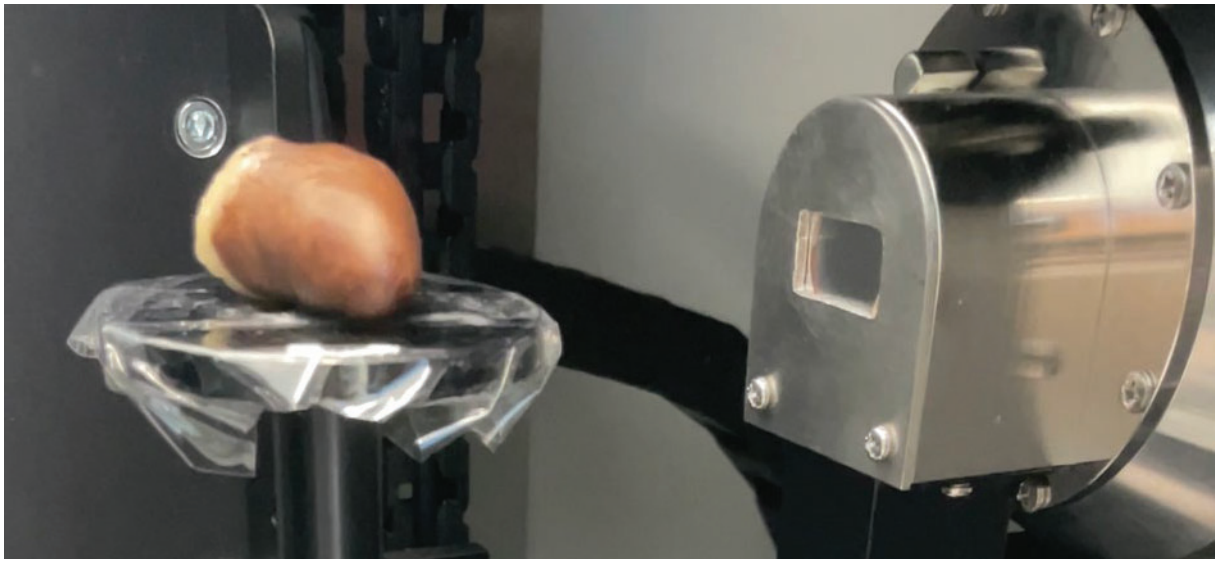

Fig. 2. The FF heart on a table. On the right side, there is an X-ray tube
Rys. 2. Serce stabilizowane formaliną na stoliku. Po prawej stronie przedstawiona jest lampa RTG

9.3. Experiments and results

The reconstructed 3D volumetric images were statistically analyzed in a Python 3.9.6 environment and visualized in 3D Slicer (https://slicer.org) software. The following parameters of the fresh and FF specimen were assessed: the heart volume, its dimensions along main axes (defined as the longest vertical and horizontal axes, and the longest axis perpendicular to the previous two), and average as well as extreme intensities. Additionally, signal-to-noise ratio (SNR) and contrast-to-noise ratio (CNR) were assessed according to the following equations [17]:

$$\mathrm{SNR} = \frac{I}{\sigma} \tag{2}$$

$$\mathrm{CNR} = \frac{|I_1 - I_2|}{\sqrt{\sigma_1^2 + \sigma_2^2}} \tag{3}$$

where I, I_1, and I_2 indicate the mean intensities of homogeneous components within the specimens, and σ, σ_1 and σ_2 are the standard deviations of these components.

In both images the heart was segmented, and its volume was classified as one of two main tissues: muscle or fat. The Otsu segmentation method was employed. Basic descriptive statistics were calculated for the tissues and background. CNR and SNR were calculated for arbitrary chosen homogenic volumes of size 2 x 2 x 2 mm.

9.3.1. Results

The fresh heart's volume was equal to 9.67 cm^3, while the FF specimen was 8.54 cm^3 (decrease of 11.67%). Muscle took 92.94% of the fresh heart and 92.50% of the FF. The remaining part of the heart was classified as fat. The dimensions of the fresh and FF organ are given in Table 2. Descriptive statistics for the image intensities were calculated and summarized in Table 3. The reconstructed voxel intensity values were not converted to the Hounsfield scale, hence the reported values remain dimensionless and their significance is useful for mutual comparison only.

Table 2

Dimensions and volumes of the specimens

	X	**Y**	**Z**	**volume**
Fresh	41.36 mm	16.61 mm	27.65 mm	9.67 cm^3
Formalin fixed	37.65 mm	16.12 mm	26.78 mm	8.54 cm^3
Change	-8.96%	-2.99%	-3.12%	-11.67%

Table 3

Descriptive statistics of the reconstructed volumes

	Fresh heart			**Formalin-fixed heart**		
	muscle	**fat**	**background**	**muscle**	**fat**	**background**
mean	43 396	37 697	25 307	40 049	33 561	19 067
std	1 276	1 145	8 643	1 434	1 494	7 245
min	36 120	31 896	0	31 906	26 448	0
max	63 057	43 893	39 227	64 550	41 457	34 194
median	43 422	37 799	28 084	40 062	33 642	21 588
SNR	1 156	1 084	9	780	505	7

Experiments revealed that all average values of the tissue intensity decreased in the FF specimen. Additionally, the differences between the mean values (i.e., the intensity contrast) increased. These features are presented in Fig. 4. Values of SNR are smaller in the FF specimen. CNR values between muscle and fat equal to 3.32 and 3.13 for fresh and FF specimens, respectively.

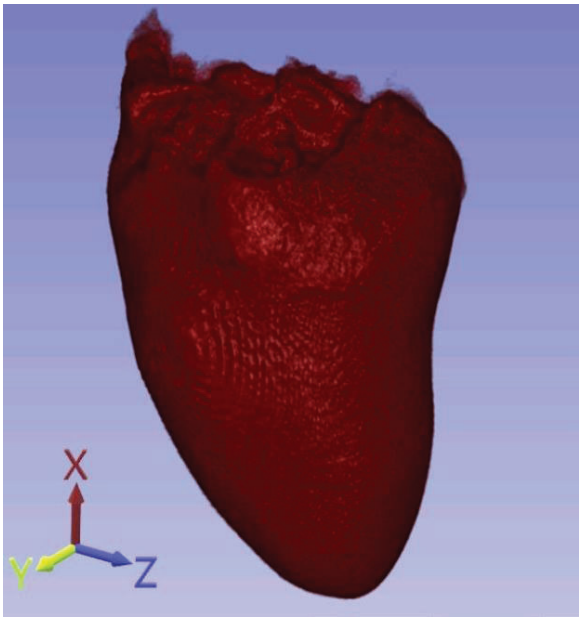

Fig. 3. Volumetric rendering of the fresh heart
Rys. 3. Wizualizacja wolumetryczna świeżego serca

The obtained results indicate that the process of formalin fixation of the poultry heart does not negatively affect the imaging of the tissue. Muscle and fat can be distinguished clearly in both images, as presented in Fig. 4 and Fig. 5. Fresh tissue is more flexible than FF specimen, hence there are motion artifacts in the reconstruction

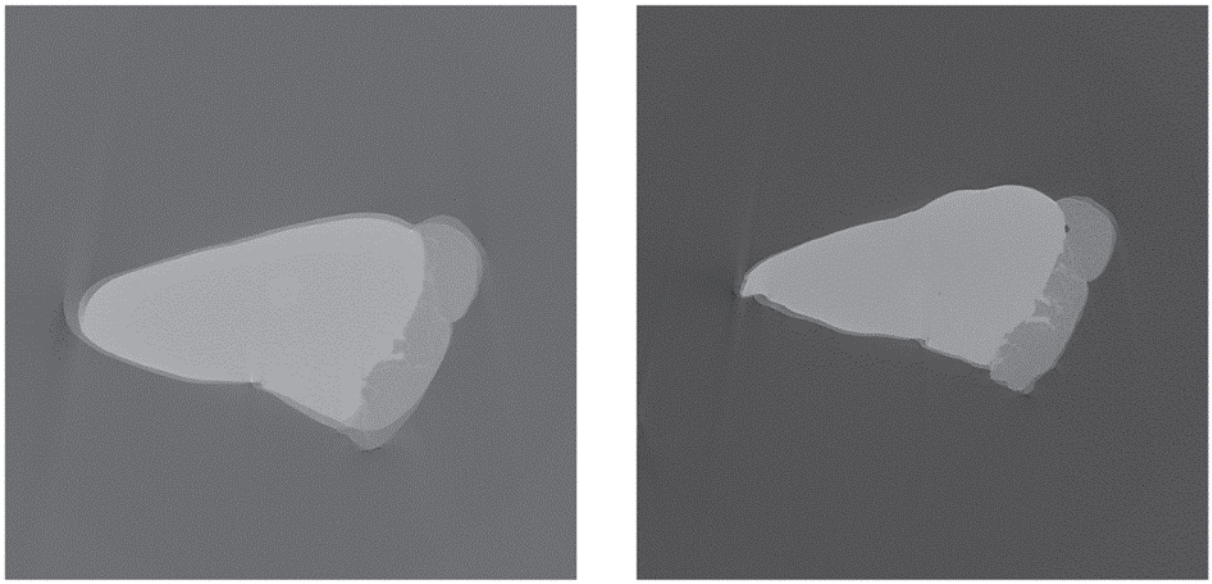

Fig. 4. Images of fresh (left) and FF (right) heart. In the FF heart, higher contrast and smaller volume may be noted. In the fresh image, movement artifacts in the most lower part of the tissue are visible.
Rys. 4. Obrazy serca świeżego (strona lewa) i stabilizowanego w formalinie (strona prawa). W obrazie serca stabilizowanego widoczny jest większy kontrast i mniejsza objętość. W obrazie serca świeżego widoczne są artefakty ruchowe w najniższym fragmencie tkanki.

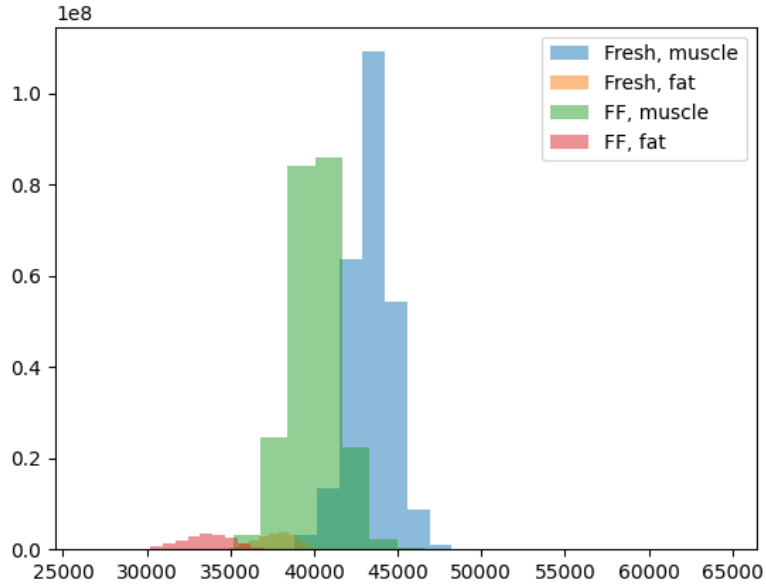

Fig. 5. Histograms of intensities of the fresh and FF heart tissues
Rys. 5. Histogram intensywności wokseli tkanek serca świeżego i stabilizowanego w formalinie (FF)

9.4. Conclusion

In the paper, 3D μCT imaging of a poultry heart was presented. The images were acquired from fresh and FF tissues. Fixation was performed in a standard way in a formaline solution. The results show that stabilization does not decrease the quality of imaging, yet slightly improves the contrast. FF images also feature significantly reduced motion artifacts. The change in the organ volume is small and regular, and does not affect the quality of the images.

Bibliography

1. Lin A.S.P., Stock S.R., Guldberg R.E.: Microcomputed Tomography, [in:] Hawkes P.W., Spence J.C.H. (eds.): *Springer Handbook of Microscopy*. Cham: Springer International Publishing, (2019): 1205–36.
2. Ritman E.L.: Current Status of Developments and Applications of Micro-CT. *Annual Review of Biomedical Engineering* (2011); **13**: 531–52.
3. Orhan K. (ed.): *Micro-Computed Tomography (Micro-CT) in Medicine and Engineering*. Cham: Springer International Publishing, (2020).

4. Larsson D.H., Vågberg W., Yaroshenko A., Yildirim A.Ö., Hertz H.M.: High-resolution short-exposure small-animal laboratory X-ray phase-contrast tomography. *Scientific Reports* (2016); **6**: 39074.
5. Betz O., Wegst U., Weide D. et al.: Imaging applications of synchrotron X-ray phase-contrast microtomography in biological morphology and biomaterials science. I. General aspects of the technique and its advantages in the analysis of millimetre-sized arthropod structure. *Journal of Microscopy* (2007); **227**: 51–71.
6. Pichat J., Iglesias J.E., Yousry T., Ourselin S., Modat M.: A Survey of Methods for 3D Histology Reconstruction. *Medical Image Analysis* (2018); **46**: 73–105.
7. Pyciński B., Yagi Y., Walts A.E., Gertych A.: 3-D Tissue Image Reconstruction from Digitized Serial Histologic Sections to Visualize Small Tumor Nests in Lung Adenocarcinomas. *Information Technology in Biomedicine*. Vol. 1186. Cham: Springer International Publishing, (2020): 55–70.
8. Rodgers G., Kuo W., Schulz G. et al.: Virtual histology of an entire mouse brain from formalin fixation to paraffin embedding. Part 1: Data acquisition, anatomical feature segmentation, tracking global volume and density changes. *Journal of Neuroscience Methods* (2021); **364**: 109354.
9. Kawata N., Teplov A., Ntiamoah P., Shia J., Hameed M., Yagi Y.: Micro-computed tomography: A novel diagnostic technique for the evaluation of gastrointestinal specimens. *Endoscopy International Open* (2021); **09**: E1886–9.
10. Scott A.E., Vasilescu D.M., Seal K.A.D. et al.: Three Dimensional Imaging of Paraffin Embedded Human Lung Tissue Samples by Micro-Computed Tomography. *PLOS ONE* (2015); **10**: e0126230.
11. Khimchenko A., Deyhle H., Schulz G. et al.: Extending two-dimensional histology into the third dimension through conventional micro computed tomography. *NeuroImage* (2016); **139**: 26–36.
12. Busse M., Müller M., Kimm M.A. et al.: Three-dimensional virtual histology enabled through cytoplasm-specific X-ray stain for microscopic and nanoscopic computed tomography. *Proceedings of the National Academy of Sciences* (2018); **115**: 2293–8.
13. Senter-Zapata M., Patel K., Bautista P.A., Griffin M., Michaelson J., Yagi Y.: The Role of Micro-CT in 3D Histology Imaging. *Pathobiology: Journal of Immunopathology, Molecular and Cellular Biology* (2016); **83**: 140–7.
14. Walton L.A., Bradley R.S., Withers P.J. et al.: Morphological Characterisation of Unstained and Intact Tissue Micro-architecture by X-ray Computed Micro- and Nano-Tomography. *Scientific Reports* (2015); **5**: 10074.

15. Teplov A., Tabata K., Fu X. et al.: Development of Standard Operating Procedure (SOP) of Micro-computed tomography (micro-CT) in Pathology. *Diagnostic Pathology* (2019); **5**.
16. Pauwels R., Jacobs R., Singer S.R., Mupparapu M.: CBCT-based bone quality assessment: are Hounsfield units applicable? *Dentomaxillofacial Radiology* (2015); **44**: 20140238.
17. Clark D.P., Ghaghada K., Moding E.J., Kirsch D.G., Badea C.T.: In vivo characterization of tumor vasculature using iodine and gold nanoparticles and dual energy micro-CT. *Physics in Medicine and Biology* (2013); **58**: 1683–704.

X-RAY MICROTOMOGRAPHY IMAGING OF FRESH AND FORMALIN-FIXED POULTRY HEART

Abstract

X-ray microtomography (μCT) is an imaging technique of growing popularity in recent years. It can visualize small samples with a resolution of the final image reaching micrometers. It remains an open question whether μCT can – to some extent – replace or complement histopathological imaging. This study aims to compare μCT images of fresh and formalin-fixed poultry heart specimens. The following features were calculated: the heart volume, its dimensions along main axes, distributions of voxel intensities. The obtained results indicated that the process of formalin fixation of the poultry heart did not negatively affect the imaging of the tissue, and muscle and fat can be distinguished clearly in the images. Fixation also reduces the severity of motion artifacts related to the shrinkage of the sample.

Keywords: X-ray microtomography, formalin-fixed tissue sample, *in-vitro* study